E. Maggiolini et alii, Frattura ed Integrità Strutturale, 33 (2015) 183-190; DOI: 10.3221/IGF-ESIS.33.23

Focussed on characterization of crack tip fields

Effective stress assessment at rectangular rounded lateral notches

Enrico Maggiolini, Roberto Tovo, Paolo Livieri
University of Ferrara
Enrico.maggiolini@unife.it, Roberto.tovo@unife.it, Paolo.livieri@unife.it

ABSTRACT Rectangular lateral notches are not common engineering components, thus little research attention has been directed towards the investigation of their stress field properties. Indeed, no in-depth investigations have been conducted to date to assess their effective stress distributions according to the effective stress definitions provided by more recent non-local approaches (i.e. critical distance, average values, implicit gradient values, etc.). In fact, the potential applications of this kind of investigation are not even particularly relevant. However, rectangular notches could provide an interesting theoretical and experimental benchmark or reference case in order to validate the effective stress definitions.
The aim of this paper is to investigate the linear elastic stress field at edges, corners and in the surrounding material of rectangular, sharp or rounded lateral notches. The consequent effective values of these notches are evaluated in relation to brittle fracture or their predicted fatigue strength values.
The main goal of this paper is to investigate the relationship between geometrical proportions and the location of critical failure points according to the definitions of effective stress proposed in the literature.

KEYWORDS. Fillet radius; Shoulder fillet; Notches; Equivalent stress; Local field; Implicit gradient.

INTRODUCTION

In practice, shoulder fillets (a shaft is a typical example) and U-notches (for example in relation to keyways) are commonly used and much researcher is being performed worldwide to understand the mechanisms underlying the geometry irregularity and the material behaviour in their near fields. Shoulder fillets are more frequently used than U-notches for reducing the weight and the volume of material; especially in high performance structures, where designers tend to introduce sudden reductions in section and thickness. A well-known problem associated with the use of notches regards their stress concentration factors. In the worst case scenario, notches can even result in a stress singularity with all its associated problems .
Neuber [1] and Peterson [2] are highly renowned in the field of ... because, more than 50 years ago, they provided the first solutions (in relation to just a few simple cases) for U-notches of different shapes. Since then, a great deal of research has been directed towards these kinds of notches, characterising them according to the depth and radius of the notch [3, 4], because because for how they are made it is mostly impossible to have a sharp edge instead of a notch radius.
Over the years, the precision of mechanical tools has increased dramatically, resulting in very small notch radii that often result in geometry singularities (considering the very high stress concentration factors that can increase the local stress to a negligible value for the application of a local study). For this reason, energy based criteria (strain energy densities [5]) and average stress field approaches (implicit gradient [6]) are becoming more important. U-notches of various shapes and under different load directions have been studied over recent years [7, 8], nevertheless the Brazilian disk has become one

of the most useful tools for studying this kind of problem in a simple way. Ever since the 1970's, the Brazilian disk has been commonly used for mixed-mode fracture testing of a cracked component [9, 10]; 30 years later, Torabi started to use a modified version of the original Brazilian disk, the U-notched Brazilian disc specimen, to understand the triaxial stress state around U-notches under mixed-mode loading [11, 12].
In the present article, the Authors investigate the geometries of different shaped U-notches, maintaining the same depth and only changing the angle of the notch axis (perpendicular to the applied force and at 45° to the applied force) and the height of the U-notch (from 0 to a height where the middle point of the notch tip is not affected by the proximity of the notch edge). In a subsequent step, another set of geometries were created by adding a fillet radius. U-notches characterised by these differing geometries were subjected to pure tensile load, and the notch tip was studied according to implicit gradient (IG) theory. Focusing on the position of the point of maximum first principal stress, and later IG, we investigated how its location changed with changing notch height. It is clear that the location of the point of maximum first principal stress is always in the notch tip due to the presence of a stress singularity; the situation is different for rounded notches, where it moves from the beginning of the fillet to the inside of the rounded part of the fillet.

THEORETICAL FRAMEWORK

The Authors present an approach capable of estimating the fatigue life of notched structures and welded joints based on an effective stress value computed numerically by solving the Helmholtz differential equation linked to the implicit gradient method [13]. Implicit gradient (IG) was originally formulated by Neuber in the 1930's [14]. The concept is that when it is not possible to use the local value of stress (due to the infinite value of the stress given by FEM in the crack tip, for example), the better way to calculate an effective local stress is to use the near stress field with a proper averaging function. The implicit gradient method supports the idea that the damage should be related to an average value of the stress components exerted on the body; when calculating this average, the stress values near to the critical point have a greater impact than the distant field (this suggests the possible use of a weight function). In other words, with a non-local approach we can determine the local effective stress and then compare it with the reference resistance. This theory is based on a differential equation resulting from the Helmholtz equation that includes a constant representing the characteristic length "c" for a weldable structure equal to 0.2 mm.

$$\sigma_{eff,IG} - c^2 \nabla^2 \sigma_{eff,IG} = \sigma_{eq} \tag{1}$$

$$\nabla^2 \sigma_{eff,IG} \cdot n = 0 \tag{2}$$

The gradient parameter "c" is a squared length; an internal length scale is therefore present in the gradient formulation (the set-up of this parameter is explained in [15]).
As shown in Eq. (1), the only variable of this equation is the equivalent stress σ_{eq}, which in our case is the first principal stress. As a result, we obtained the IG effective stress $\sigma_{eff,IG}$. Eq. (2) is the natural boundary condition [16, 17].
It is important to consider that if the first principal stress is taken as σ_{eq}, the entire study field is around the point of maximum tension, but that does not mean that the result (maximum value of $\sigma_{eff,IG}$) is necessarily in the same location. However, as will be shown below, the maximum $\sigma_{eff,IG}$ does not always match the location of maximum first principal stress, but it remains in the very near field.
The FE software COMSOL MULTIPHYSICS admits the implementation of this kind of equation.

GEOMETRIES AND MODEL PROPERTIES

Two macrosets of notch geometry were created with variable notch height. The first set is based on a horizontal notch with a fixed depth, and the second set is based on a notch of the same depth, but with the orientation of the notch set at 45 degrees. The origin is taken in the notch upper tip.
The half notch height H varies between 0 and 4.
A vertical tensile unitary load is applied to the top 25mm side, while the bottom 25mm side is fixed.
To make a proper model, we created a mesh with triangular elements and a mapped mesh zone over the notch tip. For the horizontal notch, the model was created with symmetry constraints in the mid-section of the notch.

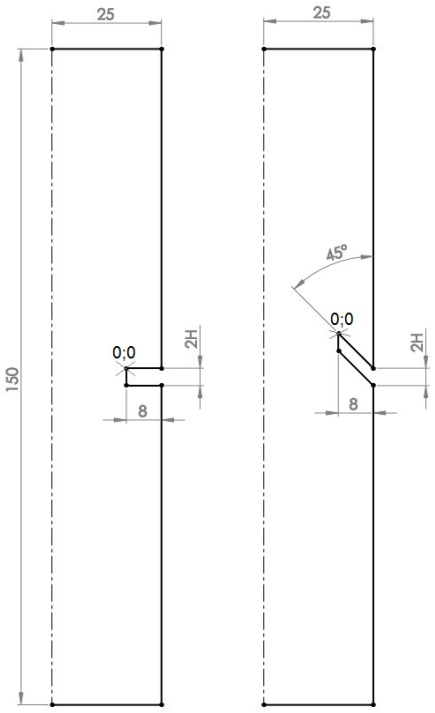

Figure 1: First two sets of notch geometries. The spotted line is a symmetry axis. Size in mm.

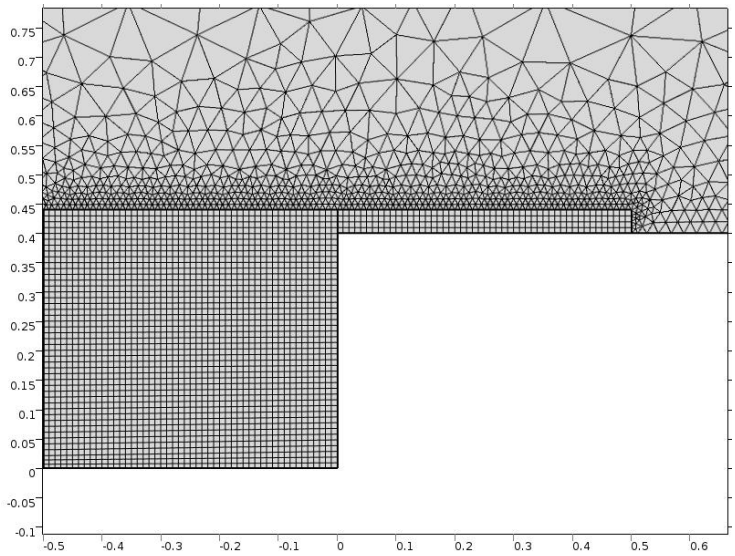

Figure 2: Mesh detail: element size=0.01 mm, H=0.4 mm.

RESULTS

The first principal stress (σ_1) in notched geometries is maximum in the tip of the notch.
As can be seen in this example, the maximum value of $\sigma_{eff,IG}$ is located in an unexpected position, and its location moves as H changes.
As concerns the horizontal notch, the maximum value of $\sigma_{eff,IG}$ is clearly located in the mid-section of the notch until H/c=1.5.
In the inclined notch, the location of maximum tension is always near the upper tip.

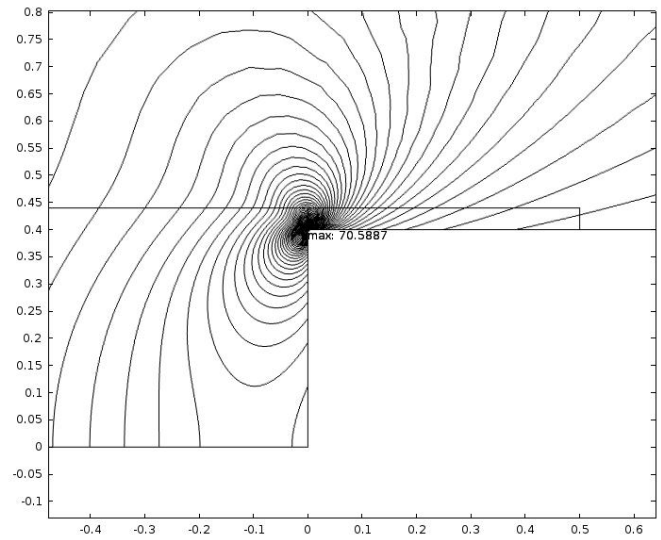

Figure 3: An isoline graph depicting first principal stress (100 lines).

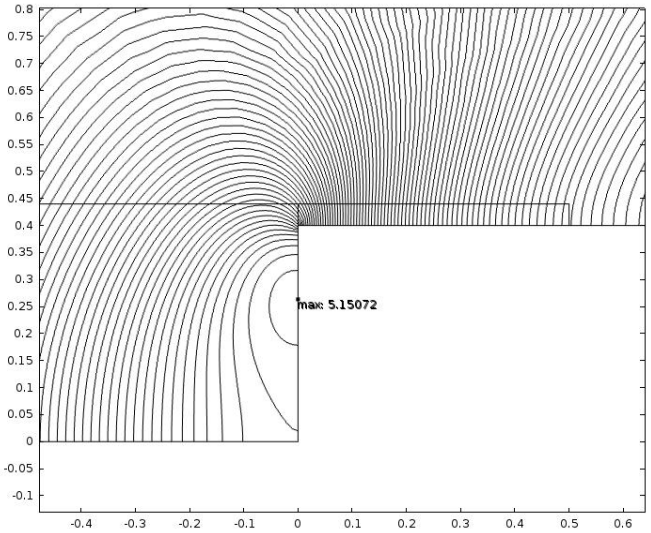

Figure 4: Example of $\sigma_{eff,IG}$ plot with isolines graph (100 lines).

	Max $\sigma_{eff,IG}$			
	Horizontal		Inclined	
H/c	x	y	x	y
0	-0.05	0.00	-0.01	-0.06
0.1	-0.02	-0.02	0.01	-0.05
0.25	0.00	-0.05	0.00	-0.09
0.5	0.00	-0.10	0.00	-0.15
1	0.00	-0.20	0.00	-0.27
2	0.00	-0.14	0.00	-0.72
4	0.00	-0.08	0.00	-1.56
6	0.00	-0.06	0.00	-0.11
10	0.00	-0.06	0.00	-0.10
20	0.00	-0.05	0.00	-0.20

Table 1: Position of the max $\sigma_{eff,IG}$ related to H/c.

We can easily create a coordinate system to locate the point of maximum stress and graph its position (curvilineal coordinate dimension d).

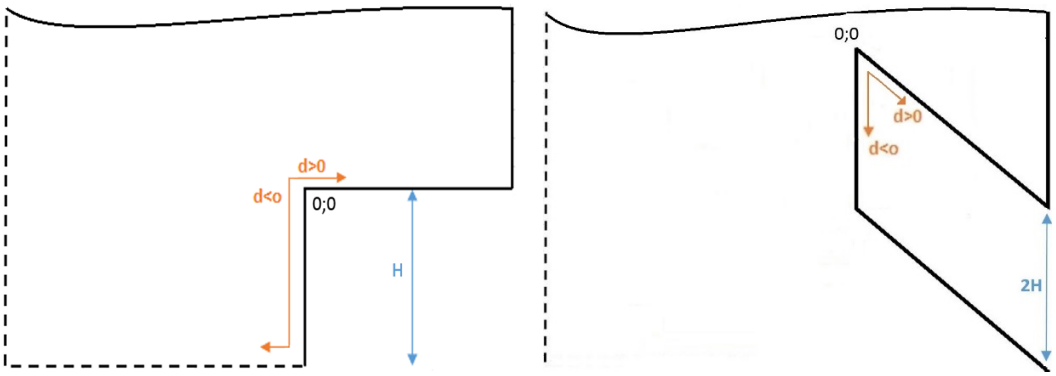

Figure 5: coordinate systems for the max tension point location.

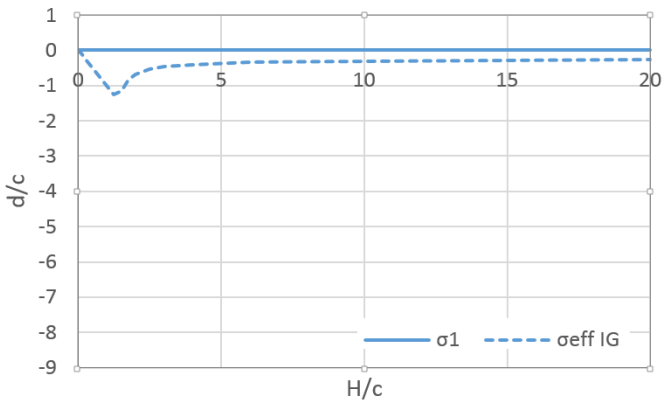

Graph 1: Tendency of the position in the horizontal notch.

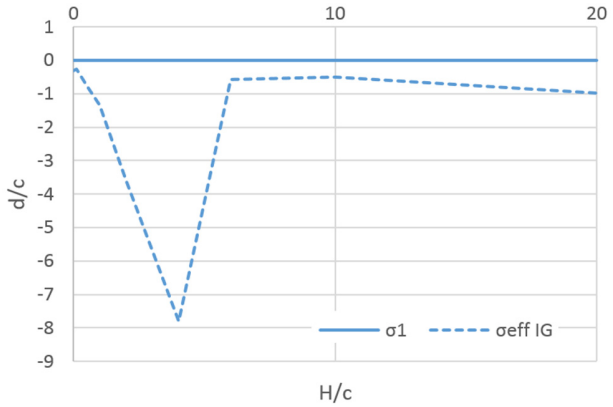

Graph 2: Tendency of the position in the inclined notch

With regards to the trend of the maximum value of $\sigma_{eff,IG}$ as a function of H/c, a trend very similar to that reported in [18] is seen, whereby it does not depend on the notch height, but on the lateral V-notch opening angle.

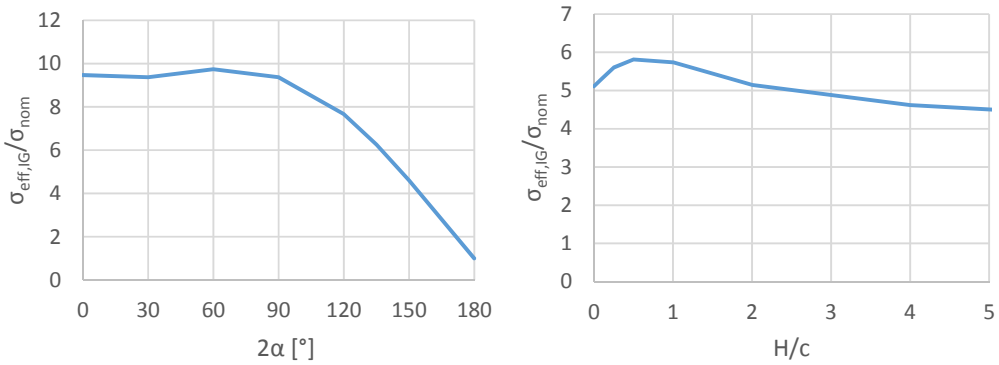

Graph 3: Trend of $\sigma_{eff,IG}$ depending on the opening angle in [18] (left) and on H/c (right)

In both cases, $\sigma_{eff,IG}$ rises until it reaches its maximum level (located at $2\alpha=60°$ and $H/c=0.05$), before falling back down to the minimum.

Second set of geometries

As concerns the notched geometries with radius, σ_1 does not reach its maximum in the point where the fillet starts, but it moves in the curvilinear part of the notch as shown in Fig. 7.

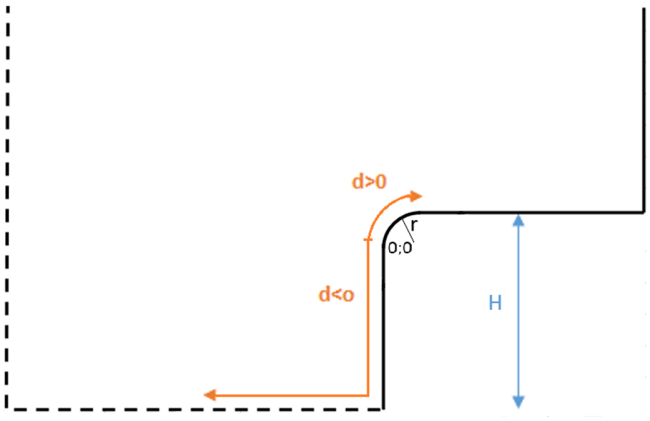

Figure 6: Coordinate system for the max tension point location.

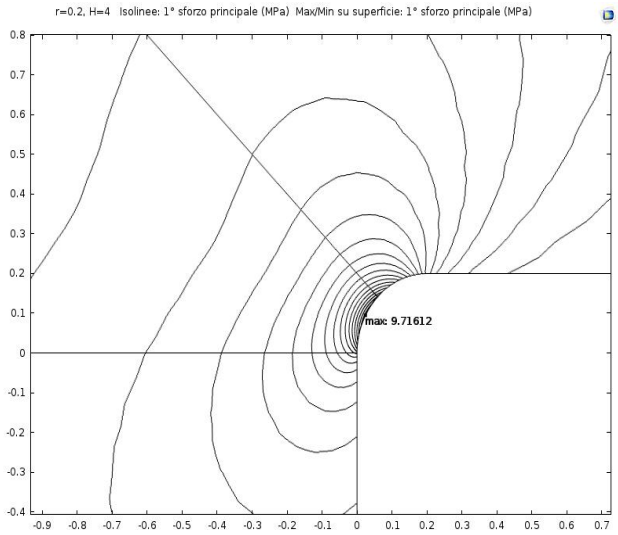

Figure 7: Example of first principal stress plot in rounded notch.

Even $\sigma_{eff,IG}$ moves around the curvilinear part of the notch, always remaining in the first half of the rounded part.

	Max. σ_1		Max. $\sigma_{eff,IG}$	
(H-r)/c	x	y	x	y
0	0.0000	0.0000	-0.0416	0.0000
0.05	0.0009	0.0040	-0.0157	-0.0100
0.45	0.0015	0.0053	0.0000	-0.0900
0.95	0.0018	0.0057	0.0000	-0.1900
1.45	0.0019	0.0058	0.0000	-0.2225
1.95	0.0019	0.0058	0.0000	-0.1263
3.95	0.0021	0.0061	0.0000	-0.0710
5.95	0.0021	0.0061	0.0000	-0.0595
9.95	0.0022	0.0062	0.0000	-0.0442
19.95	0.0022	0.0062	0.0000	-0.0443

Table 2: Position of the max. $\sigma_{eff,IG}$ and σ1 related to (H-r)/c for r=c/20.

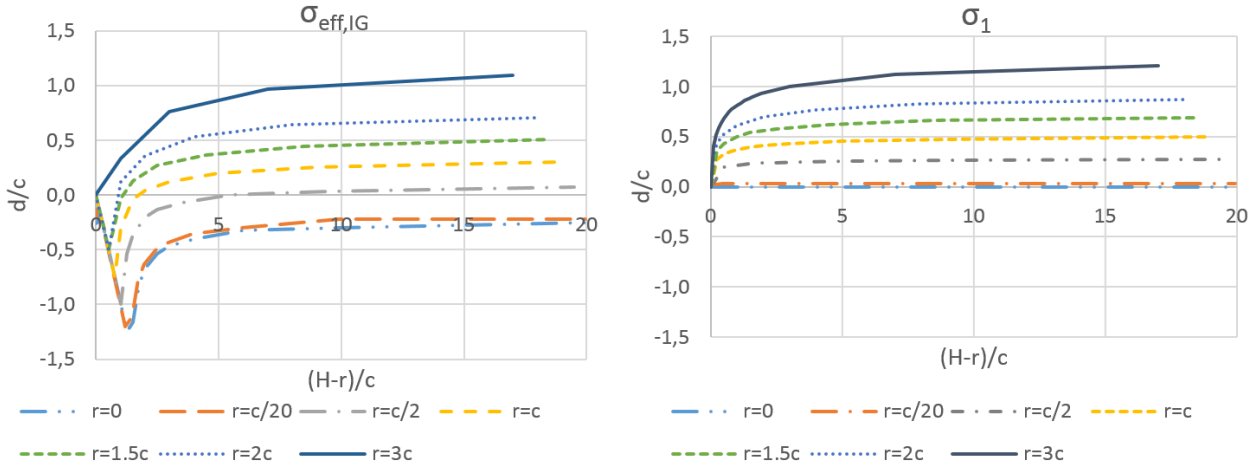

Graph 4: Tendency of the position as a function of r/c and (H-r)/c

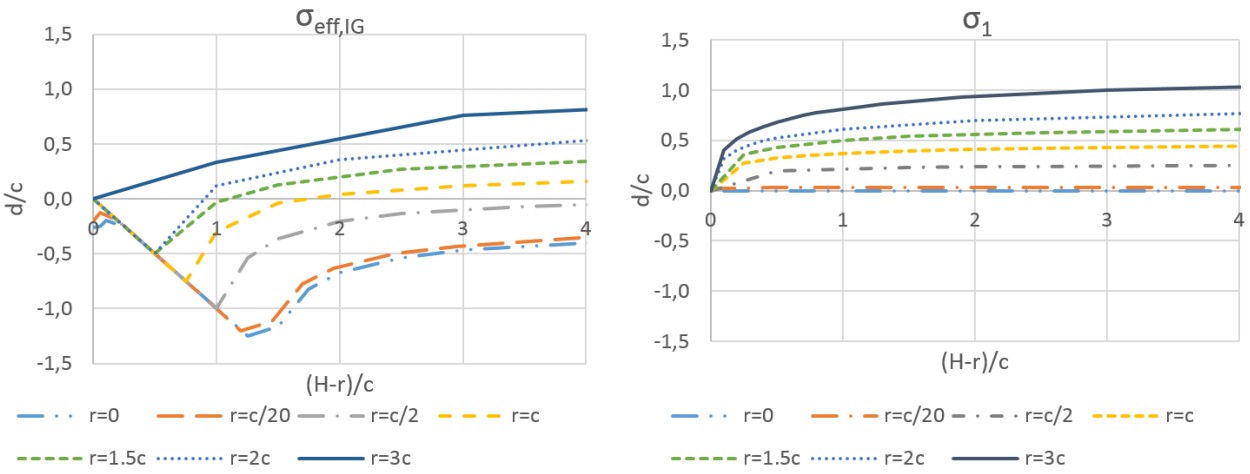

Graph 5: zooms of the Graph 4.

It is extremely difficult to consider the fillet radius in inclined notches due to the different opening angles of the two notch tips: the lower tip has an opening angle of 135° and can support almost any radius, whereas the upper tip has a very sharp angle of 45° and cannot support large radii for the lower values of H.

CONCLUSIONS

The aim of this work was to investigate how the location of maximal $\sigma_{eff,IG}$ changes with varying notch geometries as estimated using implicit gradient theory. To confirm the findings, specimens should be made and tensile tests performed to verify whether fracture initiation occurs in the same points as highlighted by this paper.
With regard to the inclined notch: as H increases, the location of maximum $\sigma_{eff,IG}$ moves up towards the sharper notch angle; for large values of H, the locations of maximal $\sigma_{eff,IG}$ concentrate in the notch tip. For the horizontal notch, on the other hand, both notch tips have the same opening angle. Graph 5 shows how the location of maximum $\sigma_{eff,IG}$ moves from the middle of the notch towards the notch tip: i.e. the rising parts after the first 45° straight line. It increases until d/c=0; this means that, in the fillet notch, the maximum tension point moves to the curvilinear parts of the notch.
In a future study, a material should be chosen, the constant "c" calculated, and a fillet radius selected; using these data and Graph 5, it will be clear how big H should be in order to have the fracture initiation point in the notch wall or in the notch tip. However, since notch size and radius are very small, it may not be clear or easy to locate the starting point of the cracks. If identification of the fraction initiation points proves to be possible, we will be able to ascertain whether the initiation point follows the implicit gradient rules, the first principal rules or neither of the two.

REFERENCES

[1] Neuber H., Kerbspannungslehre, springer, Berlin (1957).
[2] Walter D., Deborah F., Peterson's stress concentration, 3rd edition, John Wiley & Sons, Inc. (2008).
[3] Noda, N.-A., Takase Y., Monda, K., Stress concentration factors for shoulder fillets in round and flat bars under various loads, Int. J. Fatigue, 19(1) (1997) 75-84.
[4] Waldman, W., Heller, M., Chen, G.X., Optimal free-form shapes for shoulder fillets in flat plates under tension and bending, International Journal of Fatigue, 23 (2001) 509–523.
[5] Torabi, A.R., Berto, F., Strain energy density to assess mode II fracture in U-notched disk-type graphite plates, Int. Journal of Damage Mechanics, 23(7) (2014) 917-930.
[6] Maggiolini, E., Livieri, P., Tovo, R., Implicit gradient and integral average effective stresses: Relationships and numerical approximations, Fatigue and Fracture of Engineering Materials and Structures, in press, (2014).
[7] Zappalorto, M., Lazzarin, P., Stress fields due to inclined notches and shoulder fillets in shafts under torsion, Journal of Strain Analysis for engineering design, 46 (2011).

[8] Majima, T., Tobita, T., Kimizuka, Y., Experimental Investigation on Interference Effect of Notch on Strength of Notched Bar with Double U-Notches of Unequal Depth and Radius, Zairyo/Journal of the Society of Materials Science, Japan, 36(407) (1987) 871-877.
[9] Awaji, H., Sato, S. Combined mode fracture toughness measurement by the disc test, J. Engng. Mater. Tech., 100 (1978) 175–182.
[10] Awaji, H., Kato, T., Griffith criterion for mode II fracture of ceramics, Experimental Mechanics, Alison, Balkema, Rotterdam, (1978) 1199–1204.
[11] Torabi, A.R., Fakoor, M., Pirhadi, E., Fracture analysis of U-notched disc-type graphite specimens under mixed mode loading, International Journal of Solids and Structures, Manuscript Draft, IJSS-D-13-00336.
[12] Torabi, A.R., Berto, F., Strain energy density to assess mode II fracture in U-notched disk-type graphite plates, International Journal of Damage Mechanics, 23(7) (2014) 917–930.
[13] Tovo, R., Livieri, P., An implicit gradient application to fatigue of sharp notches and weldments, Engineering Fracture Mechanics, 74 (2007) 515–526.
[14] Neuber: Theory of Notch Stresses, Springer-Verlag, Berlin (1958).
[15] Tovo, R., Livieri, P., An implicit gradient application to fatigue of sharp notches and weldments, Engineering Fracture Mechanics, 74 (2007) 515–526
[16] Lasry, D., Belytschko, T., Localization limiters in transient problems, Inf. J. Solids Struct., 24 (1988) 581–597.
[17] Miihlhaus, H.-B., Aifantis, E. C., A variational principle for gradient plasticity, Int. J. Solids Struct., 28 (1991) 845–857.
[18] Maggiolini, E., Livieri, P., Tovo, R., On Numerical Integration for Effective Stress Assessment at Notches, Frattura ed Integrità Strutturale, 25 (2013) 117-123; DOI: 10.3221/IGF-ESIS.25.17.